Examination of Northeast U.S. Ozone Concentrations in the Widest Possible Temporal and Spatial Context

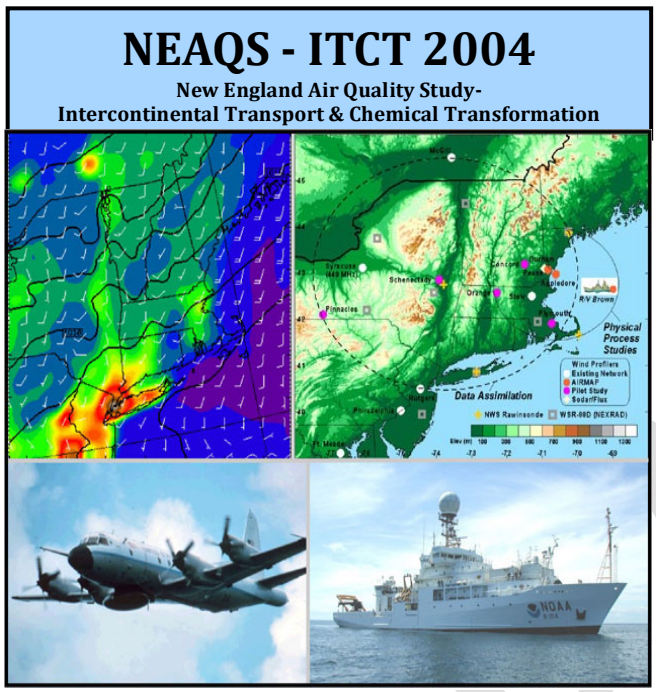

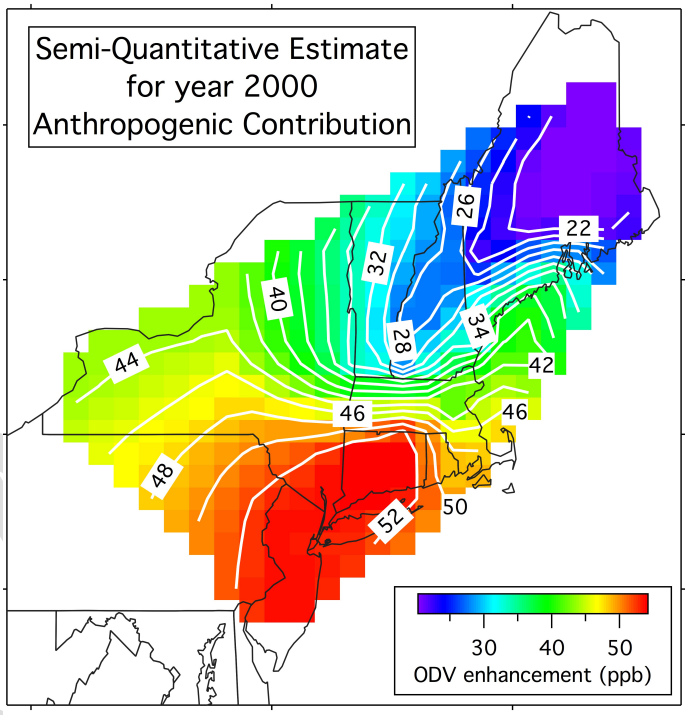

Final Report to Northeast States for Coordinated Air Use Management, Inc. (NESCAUM)

David D. Parrish
David.D.Parrish, LLC
Boulder, Colorado, 80304

DRAFT
15 September 2017

Cover Figure

(Left) Overview of NOAA instrumentation deployed for the ICARTT field study (figure from NOAA/ ESRL/CSD website). (Right) Contour plot of the enhancement of ozone design values in the NESCAUM region due to photochemical production from anthropogenic emissions; values are estimates for the year 2000. This figure is included in the report as part of Figure 23.

Disclaimer

The preparation of this report was financed by a contract from New York State Energy and Research Development Authority (NYSERDA) through Northeast States for Coordinated Air Use Management, Inc. (NESCAUM). The content, findings, opinions and conclusions are the work of the author and do not necessarily represent findings, opinions or conclusions of NYSERDA or NESCAUM.

Acknowledgements

This Report was submitted in fulfillment the Technical Services Agreement between NESCAUM and David.D.Parrish, LLC funded by PO# ERDA1-00000108471, Task Work Order No. 2 (NESCAUM project# 2393), issued by NYSERDA.

1.0 INTRODUCTION

The goal of this study is two-fold. First, provide an examination of the data sets from the NOAA contribution to the ICARTT 2004 study; the emphasis here is on the analyses most relevant to understanding air quality and pollutant transport downwind of the New York City metropolitan area, and directing readers to specific papers for further details. Second, give a preliminary examination of the existing record of ozone design values measured in the NESCAUM states (Connecticut, Maine, Massachusetts, New Hampshire, New Jersey, New York, Rhode Island and Vermont) in the widest possible temporal and spatial context. The remainder of this introduction and Sections 2 through 4 address the first goal, while Sections 5 and 6 address the second.

1.1 Introduction to the ICARTT 2004 study

In the summer of 2004, several separate field programs intensively studied the photochemical, heterogeneous chemical and radiative environment of the troposphere over the northeastern U.S. and outflow regions to the North Atlantic Ocean. An international team of scientists, representing over 100 laboratories, collaborated under the International Consortium for Atmospheric Research on Transport and Transformation (ICARTT) umbrella to coordinate the separate field programs in order to maximize the resulting advances in our understanding of regional air quality, the transport, chemical transformation and removal of aerosols, ozone, and their precursors during intercontinental transport, and the radiation balance of the troposphere. Participants utilized nine aircraft, one research vessel, several ground-based sites in North America and the Azores, a network of aerosol-ozone lidars in Europe, satellites, balloon borne sondes, and routine commercial aircraft measurements [*Fehsenfeld et al.,* 2006]. The results of this study comprised two special issues of *Journal of Geophysical Research-Atmospheres* (Part 1, v111, D23 and part2, v112, D10).

The National Oceanic and Atmospheric Administration (NOAA) was most active in deploying platforms in the Northeast U.S. under a separate acronym (NEAQS - ITCT 2004 - see cover figure); the focus here will be primarily on the results from this agency. The NOAA platforms included:

- WP-3D aircraft - in situ measurements
- DC-3 aircraft - downward looking ozone and aerosol lidar
- Research Vessel Ronald H. Brown
- Five air quality surface sites (AIRMAP) located in northeastern United States
- 11 site radar wind profiler network

The NOAA field study had an acronym separate from ICARTT, with the platforms illustrated in the left panel of the Cover Figure. Figures 1 - 3 show the flight and cruise tracks of the aircraft and ship platforms.

The following discussion gives a general overview of the ICARTT results regarding transport and photochemical processing of ozone precursors emitted in the northeastern U.S. Illustrations of these processes focus on 20 and 21 July, when the most intense pollution event of the ICARTT period occurred.

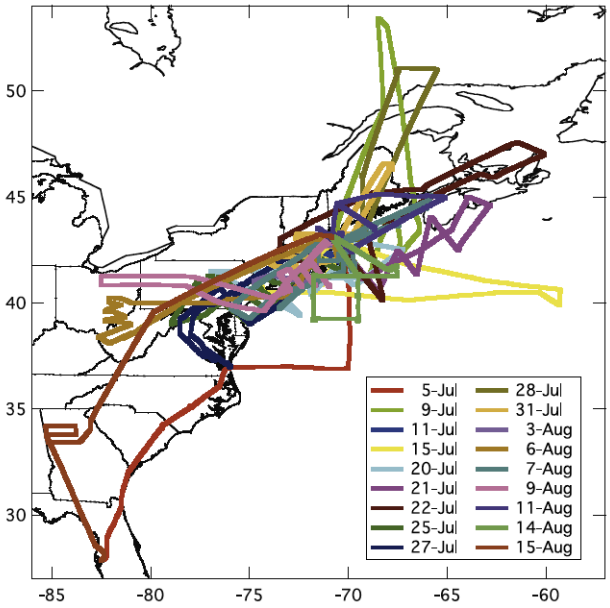

Figure 1. Flight tracks of NOAA WP-3D aircraft during ICARTT. (Figure from *Fehsenfeld et al*., 2006).

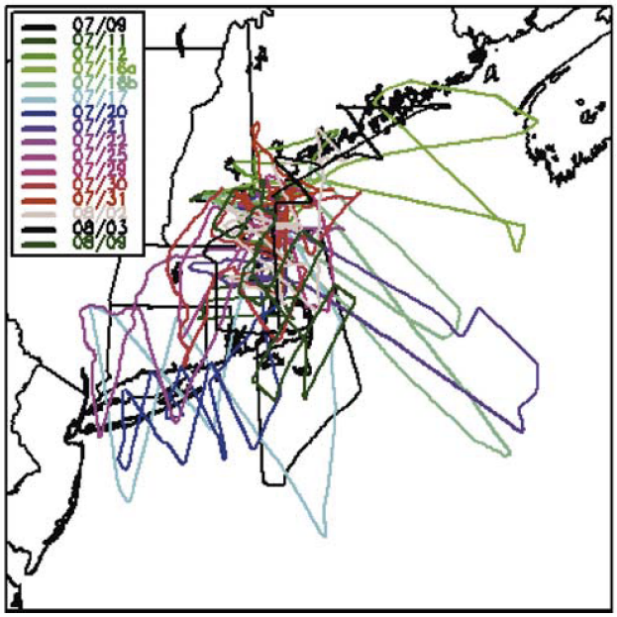

Figure 2. Flight tracks of NOAA DC-3 lidar aircraft during ICARTT. (Figure from *Fehsenfeld et al*., 2006).

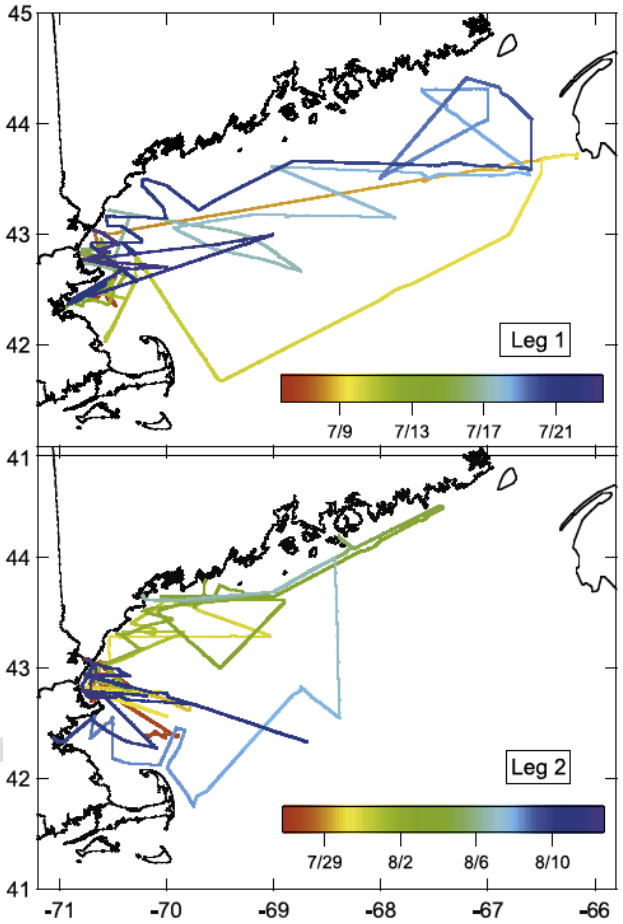

Figure 3. Cruise tracks of NOAA R/V Ronald H. Brown during ICARTT. (Figure from *Fehsenfeld et al*., 2006).

1.2 Meteorological and Precursor Context of ICARTT 2004

The meteorology that prevails during a field campaign generally exerts a profound effect upon the resulting data set, and thus those data must be interpreted within that

meteorological context. Meteorology strongly affects transport patterns and stagnation conditions as well as important parameters such as radiation intensity and ambient temperature. *White et al.* [2006] compared the July–August 2004 ICARRT period to 1996–2005 summers. They note that 2004 recorded the minimum number of ozone exceedances in New England, which was appreciably cooler and wetter than normal.

Figure 4 [*Fehsenfeld et al.,* 2006] provides a spatial and temporal context for the 2004 ozone and CO distributions measured during ICARTT, and also provides a benchmark for quantifying systematic changes that have occurred in these distributions over the 13 years since the ICARTT study. This figure presents the 2004 ozone and CO vertical profiles measured routinely on commercial aircraft by the MOZAIC program over the eastern United States and over Germany, and compares those measurements with an average of all MOZAIC measurements from previous years. The general features of these vertical profiles - increasing ozone and decreasing CO with altitude - represent the general northern mid-latitude distributions of these two species. Particular pollution features of interest observed during ICARTT and other studies are observed superimposed on these average vertical profiles.

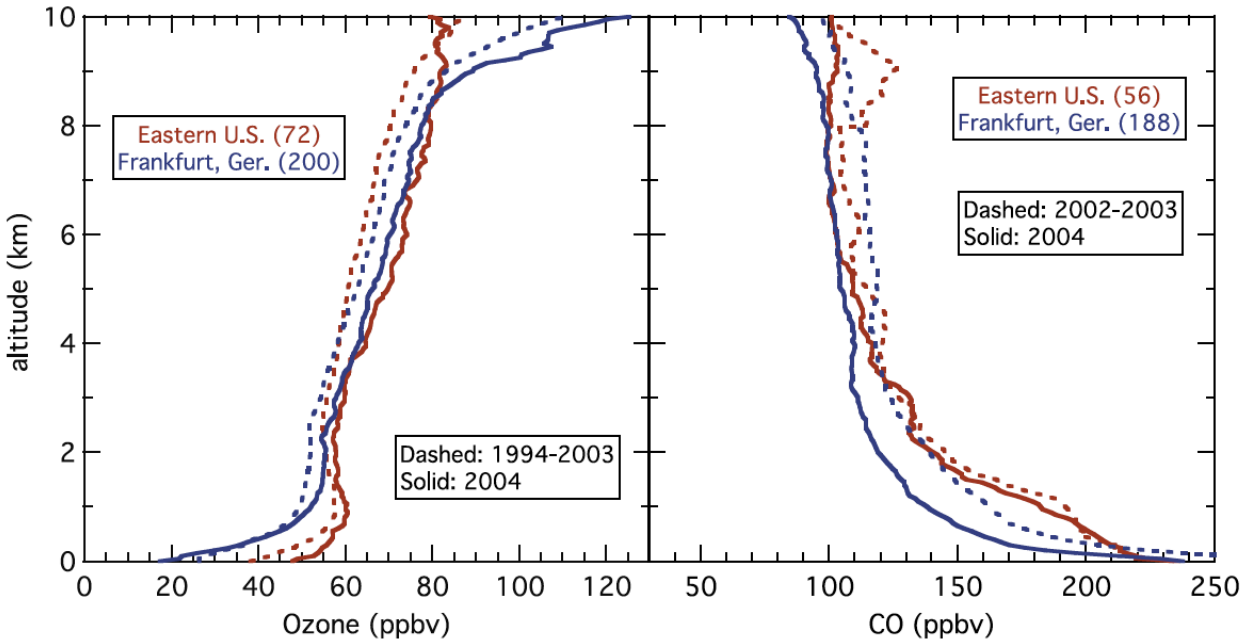

Figure 4. Average vertical profiles of ozone and CO for July–August measured by the MOZAIC program. Solid lines indicate 2004 data, and dashed lines indicate the average of all earlier years of measurements (1994–2003 for ozone and 2002–2003 for CO). Eastern U.S. represents the average from all flights into New York City, Boston, and Washington, D. C. The numbers in parentheses give the number of vertical profiles averaged in each curve for 2004. (Figure from *Fehsenfeld et al*., 2006).

2.0 TRANSPORT OVER THE GULF OF MAINE

A shallow (~50 m), stable marine boundary layer (MBL) is ubiquitous over the cool waters of the Gulf of Maine in summer; a similar situation is expected to exist in Long Island Sound, although it has been less studied. This feature profoundly affects pollutant transport throughout the marine environment abutting New York and New England; as a result, pollution transport over marine areas is very different from pollutant transport over land, with which we are more familiar. The stable MBL isolates flow aloft from the surface, leading to layered flow with strong, altitude dependent velocity and direction shear. Over land, where pollution plumes generally originate, turbulence due to convection driven by surface heating serves to homogenize flow through the depth of the convective boundary layer.

Angevine et al. [2006] find that the temperature profile of the lowest 1–2 km of the atmosphere over the Gulf of Maine is remarkably similar regardless of transport time over water or the time of day when the flow left the land, provided only that the flow is offshore. This similarity is forced by the (roughly) constant water temperature and the (roughly) constant temperature of the free troposphere over the continent. However, the processes leading to the similar profiles are quite different depending on the time of day when the flow crosses the coast. Air leaving the coast at night already has a stable profile, whereas air leaving the coast at midday or afternoon has a deep mixed layer. *Angevine et al.* [2006] show that the formation of the stable layer, which involves cooling a roughly 50- to 100-m-deep layer by 5–15 K, occurs within 10 km and a half hour after leaving the coast.

Once polluted air leaves the continent, decoupling of flow aloft from the MBL allows transport in the elevated, isolated layers to be quite efficient. In particular, emissions from the urban corridor of the northeastern United States can be efficiently transported long distances [*Neuman et al.,* 2006 and references cited therein]. Large concentrations of urban pollution routinely reach the coast of Maine, hundreds of kilometers from concentrated sources. Transport as far as Europe in the lower atmosphere has been observed.

The most favorable episode for the study of pollution transport from urban areas in the Northeast U.S. during the ICARTT period occurred on 20 and 21 July (Figures 5 and 6) when the New York City (NYC) plume was transported to the northeast. This transported plume was sampled by both the in situ measurements aboard the WP-3D aircraft and the DC-3 lidar aircraft. Figure 5 shows the flight tracks of the WP-3D aircraft with the intercepted plume indicated to the northeast of NYC by enhanced CO concentrations. The plume was tracked as far downwind as south of Nova Scotia at a distance of >1000 km from the city.

The transport of pollution from continental to marine environments results in characteristic average vertical profiles of pollutants, as illustrated in Figure 6 for ozone, CO and NOy. The overall profiles of ozone and the precursors are qualitatively consistent with

the MOZAIC profiles included in Figure 4. Ozone generally increases with altitude in both figures, but the ICARTT data show a multitude of many more enhanced concentrations below ~1.5 km. These enhancements indicate interception of pollution plumes in the lower troposphere. The profiles of the other two species, representing primary emissions, decrease with altitude consistent with the surface location of the most important emission sources, again with plumes of enhanced concentrations below 1.5 km. There are also occasional enhancements of all three species at higher altitudes, which for CO and ozone are attributed to plumes from distant wildfires transported to the Northeast U.S. above 3 km.

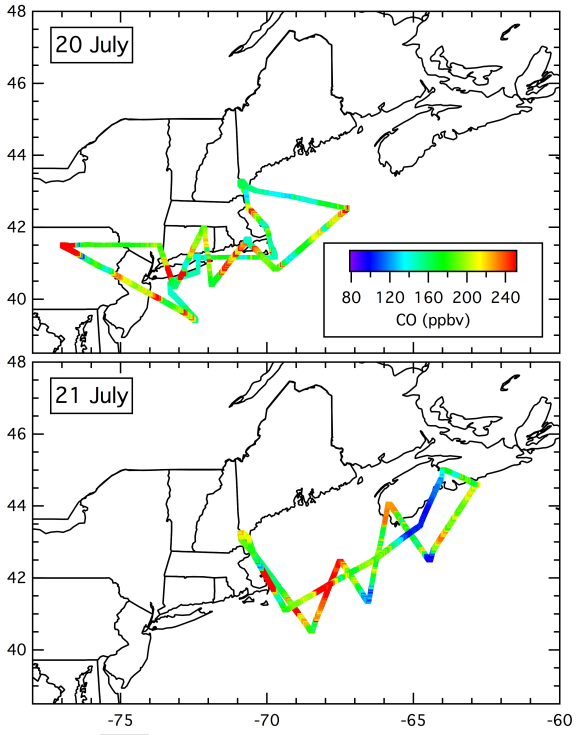

Figure 5. Flight tracks of the NOAA WP-3D aircraft on two July days during ICARTT. Each flight track is color-coded according to measurements of CO, with the warm colors indicating interception of the transported NYC plume.

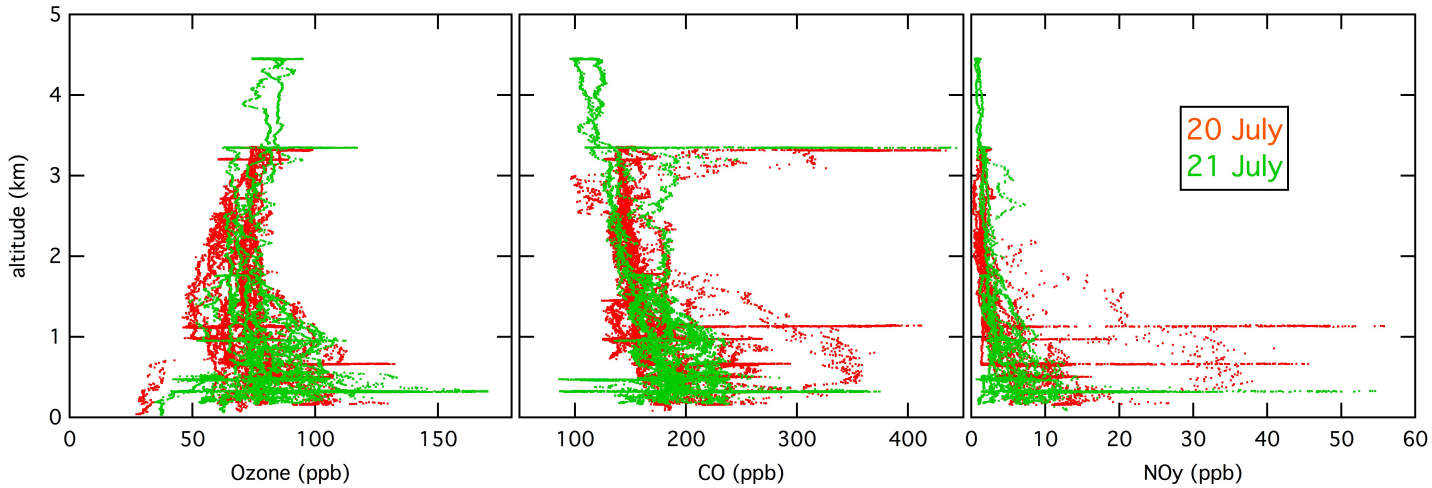

Figure 6. Vertical profiles of 1-sec average measurements of ozone, CO and NOy for two July flights of the NOAA WP-3D aircraft during ICARTT.

Lee et al. [2011] present a detailed analysis of the transport and photochemistry of the 20 and 21 July period, which includes WRF-Chem photochemical modeling. Figure 7 shows their analysis of the ozone lidar data from the DC-3 aircraft. The ozone produced within the plumes transported from NYC is clearly apparent in both the horizontal (upper figure panels) and in the vertical distributions (lower figure panels). Qualitatively, the pollution

plumes transported from NYC are well defined by the data from both aircraft platforms. However, the transport has very complex details, which *Lee et al.* [2011] discuss in the context of their photochemical modeling; some of those details include:

- The measured urban plumes extended vertically up to about 2 km near New York City, but not as high (1–1.5 km) over the stable marine boundary layer (MBL) over the North Atlantic Ocean.

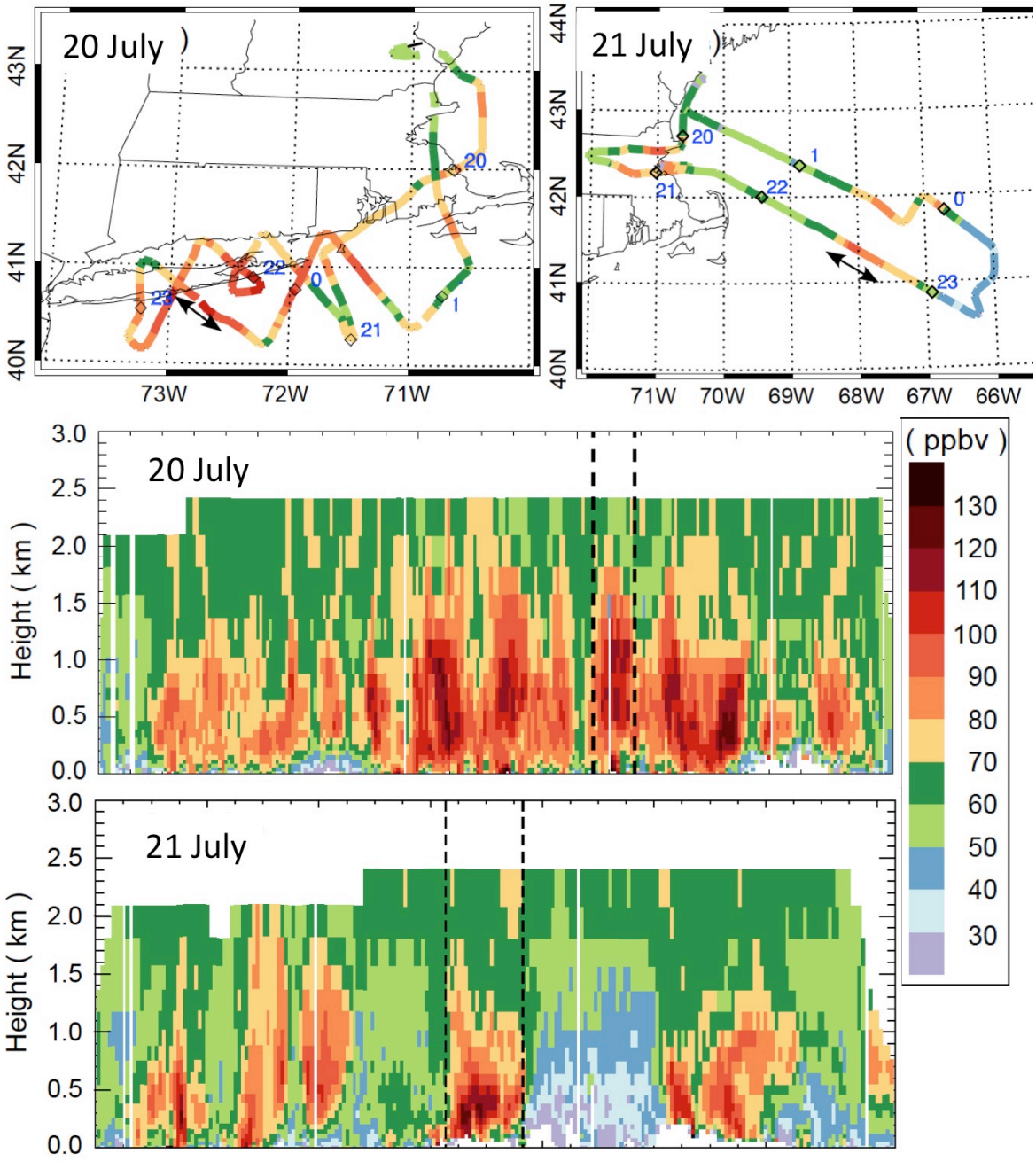

Figure 7. (top) Flight tracks of the DC-3 aircraft on 20 and 21 July color-coded by measured ozone mixing ratios vertically averaged from near surface to about 1.5 km. (bottom) Vertical distributions of observed ozone mixing ratios during the flights. The double-headed arrows in the upper plots correspond to the periods between the dashed lines in the lower plots. (Figure adapted from *Lee et al.*, 2011).

- Generally, a steep gradient is seen below about 0.5 km in the WP-3D profiles observed by in situ measurements, indicating that the urban plume is decoupled from the MBL (e.g., see Fig. 6a of *Lee et al.* [2011]), consistent with the above discussion. (This structure is not clear in the lower panels of Figure 7 above, as it is partially washed out by the vertical resolution of the ozone lidar; those data were analyzed with 450 m vertical averaging to improve the signal-to-noise in the figure.)
- The similarity of ozone concentrations measured near the source regions on July 20 and measured far downwind on July 21 indicates that the ozone plumes were efficiently transported in the lower atmosphere over the North Atlantic Ocean without significant influence of ozone loss processes. The WRF-Chem modeling nicely reproduces this feature.
- The layered structure of the lower troposphere in the marine environment results in a great deal of complexity in transport, which is driven by the vertical shear in wind speed and direction. Figures 9 - 13 of *Lee et al.* [2011] show this complexity in great detail, with a continental plume well defined in the horizontal and vertical, separating into separate plumes transported in different directions at different altitudes after entering the marine environment.

3.0 SOME ASPECTS OF PHOTOCHEMICAL PROCESSING OF URBAN POLLUTION AND RESULTING RELATIONSHIPS BETWEEN SPECIES

A great many papers (68 in the two special issues of *Journal of Geophysical Research - Atmospheres* and others since the 2007 date of those issues) have been published describing analysis of the ICARTT results. It is not our intent to review or even give a broad overview of all of this work; *Fehsenfeld et al.* [2006] have given such an overview. Here we summarize some results that may be of most relevance to analysis of more recent studies in the Northeast U.S.

During transport of pollution in isolated plumes above the ocean, ozone production can be sustained by recycling of NOx from nitric acid (HNO_3), a species generally considered to be photochemically unreactive. *Neuman et al.* [2006] investigated the photochemical and transport processes involving reactive nitrogen compounds within isolated plumes near source regions and at distances up to 1000 km downwind from the North American east coast (Figure 8). These plumes were primarily confined below 1.5 km altitude in well-defined layers, but were isolated from the ocean surface by the shallow MBL discussed earlier. In aged plumes located over the North Atlantic Ocean, HNO_3 mixing ratios were large (often 10 to 50 ppb), and HNO_3 accounted for the large majority of reactive nitrogen species (NOy). Plume CO and NOy enhancement ratios were very similar to those observed in fresh pollution near Boston and NYC, indicating efficient transport of HNO_3 without significant depositional loss. Box model calculations indicate that photolysis and OH oxidation of >10 ppb of HNO_3 that was in the troposphere for days resulted in reformation of hundreds of ppt of NOx, which is sufficient to maintain photochemical ozone production. Efficient transport of HNO_3 over the North Atlantic Ocean for days carried both HNO_3 and NOx far from their continental sources and increased their photochemical influence.

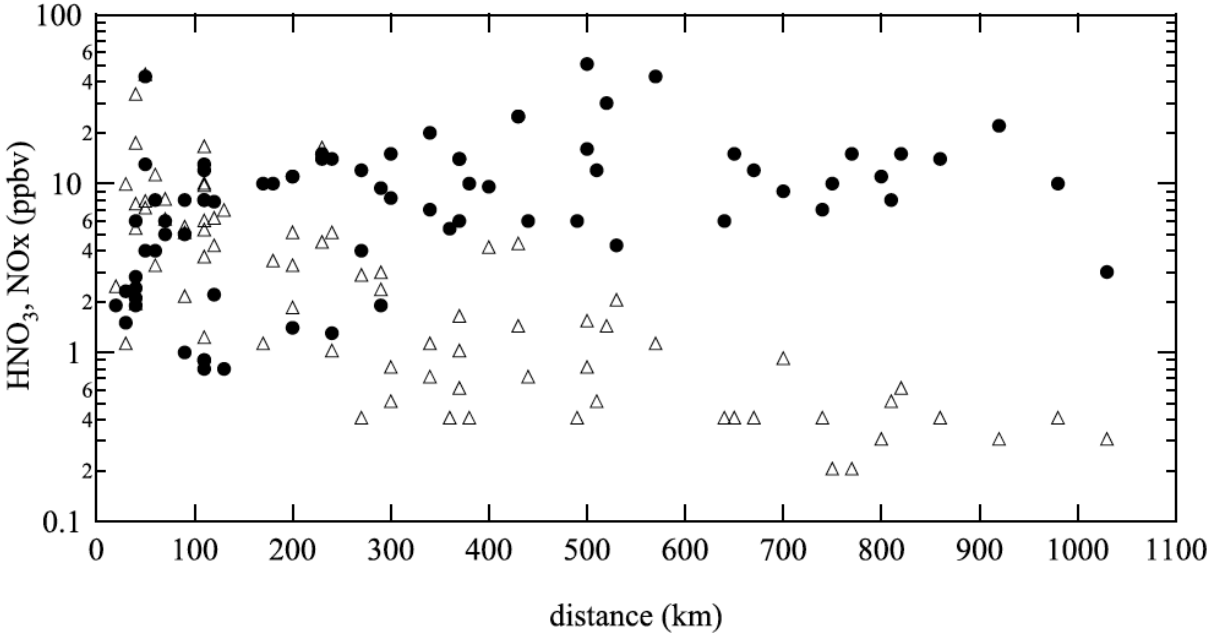

Figure 8. Maximum values of HNO_3 (solid circles) and NOx (open triangles) measured in plumes as a function of distance from the urban source. (Figure from *Neuman et al.*, 2006).

Transport of wildfire plumes can significantly enhance CO concentrations in urban areas. During the ICARTT study period, large wildfires were burning in Alaska and Canada, and some of their emissions were transported to the northeastern U.S., where they were measured by the NOAA WP-3 aircraft and the NOAA research vessel Ronald H. Brown. Using acetonitrile and chloroform as tracers of the biomass burning and the anthropogenic emissions, respectively, *Warneke et al.* [2006] determined the relative contributions from these two source classes. Even in the northeastern U.S., which is a center of intense anthropogenic emissions, approximately 30% of the measured CO enhancements within the region were attributed to transported emissions from the forest fires in Alaska and Canada, with the remaining 70% attributed to the urban emissions from mainly New York and Boston (Figure 9). On some days, the forest fire emissions were mixed down to the surface and dominated measured CO enhancements. The measurements compared well with dispersion-transport modeling, which indicated that the total emissions during the measurement campaign from biomass burning was about 22 Tg. For comparison, the U.S. EPA NEI-99 inventory gives the total U.S. anthropogenic CO emissions over the same time period as 25 Tg; however the modeling suggests that these anthropogenic emissions are over estimated by about 50%.

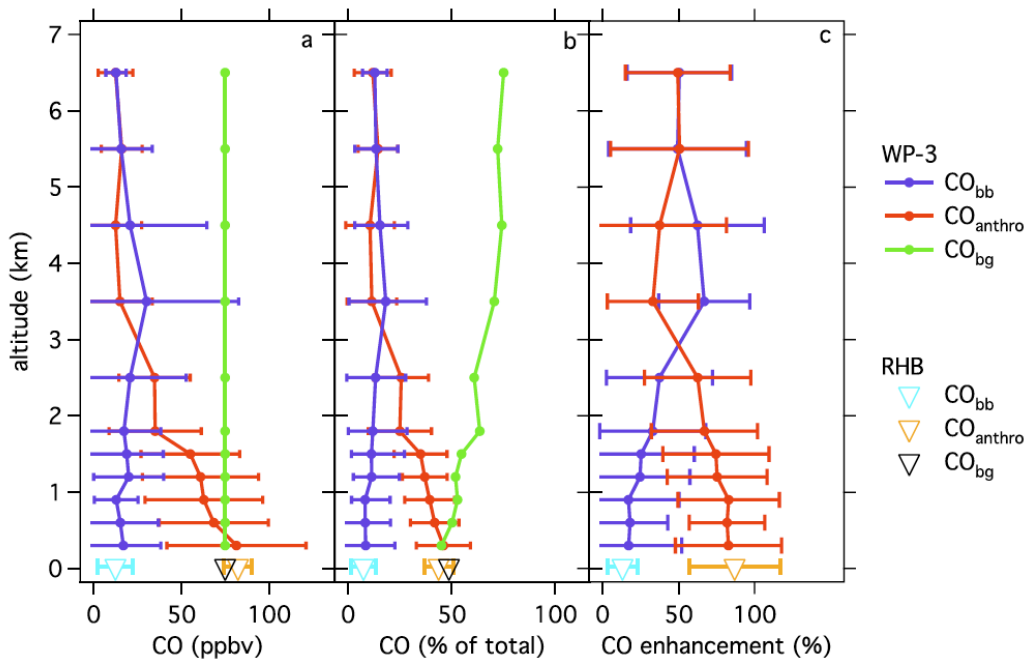

Figure 9. Average altitude profile of the three contributions to measured CO concentrations: biomass burning (CO_{bb}), anthropogenic emissions (CO_{anthro}) and background (CO_{bg}), which is approximated as 75 ppb. The error bars are the standard deviation within each altitude bin. The NOAA Ronald H. Brown measurements are indicated with the open triangles in each altitude profile. (Figure from *Warneke et al.*, 2006).

Ambient measurements can provide critical tests of relative magnitudes of atmospheric emissions of important volatile organic compounds (VOCs). During the ICARTT campaign, anthropogenic VOCs and CO were measured downwind from New York City and Boston. *Warneke et al.* [2006] calculated the emission ratios of VOCs relative to CO and acetylene using a method in which the ratio of a VOC to acetylene is plotted versus the photochemical

age. The intercept at the photochemical age of zero gives the emission ratio. The so determined emission ratios were compared to other measurement sets, including data from the same region in 2002, canister samples collected inside New York City and Boston by other researchers (Figure 10), aircraft measurements from Los Angeles in 2002, and the average urban composition of 39 U.S. cities determined in the 1980s. All the measurements generally agree within a factor of two. The measured emission ratios also agree for most compounds within a factor of two with vehicle exhaust data indicating that a major source of VOCs in urban areas is automobiles. A comparison with an anthropogenic emission database shows less agreement. Especially large discrepancies were found for the C_2-C_4 alkanes and most oxygenated species. As an example, the database overestimated toluene by almost a factor of three, which caused an air quality forecast model (WRF-CHEM) using this database to over predict the toluene mixing ratio by a factor of 2.5. On the other hand, the overall reactivity of the measured species and the reactivity of the same compounds in the emission database were found to agree within 30%.

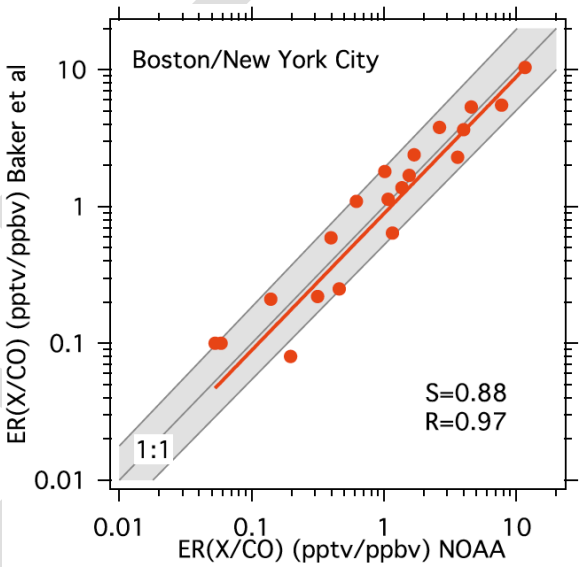

Figure 10. Comparison of VOC to CO emission ratios determined from the ICARTT data with those from *Baker et al.* [2008], which are from canister samples collected in Boston and New York City. Each data point represents one compound, and the solid red line is a linear fit through the data. The grey shaded area shows agreement within a factor of two.

Ambient measurements can also provide critical information regarding the temporal dependence of relative emission rates of species in urban areas. *Hassler et al.* [2016] examined long-term atmospheric NOx/CO enhancement ratios in megacities to provide evaluations of global emission inventories, and to demonstrate that motor vehicle emissions controls were largely responsible for U.S. urban NOx/CO trends in the past half century. Figure 11 shows some of the determinations used in this study, which include data from NYC and Boston collected during ICARTT (2004), NARE (1993) and a recent 2015 airborne study. A global inventory widely used by global chemistry models fails to capture these long-term trends and regional differences in U.S. and Europe megacity NOx/CO enhancement ratios, possibly contributing to these models' inability to accurately reproduce observed long-term changes in tropospheric ozone.

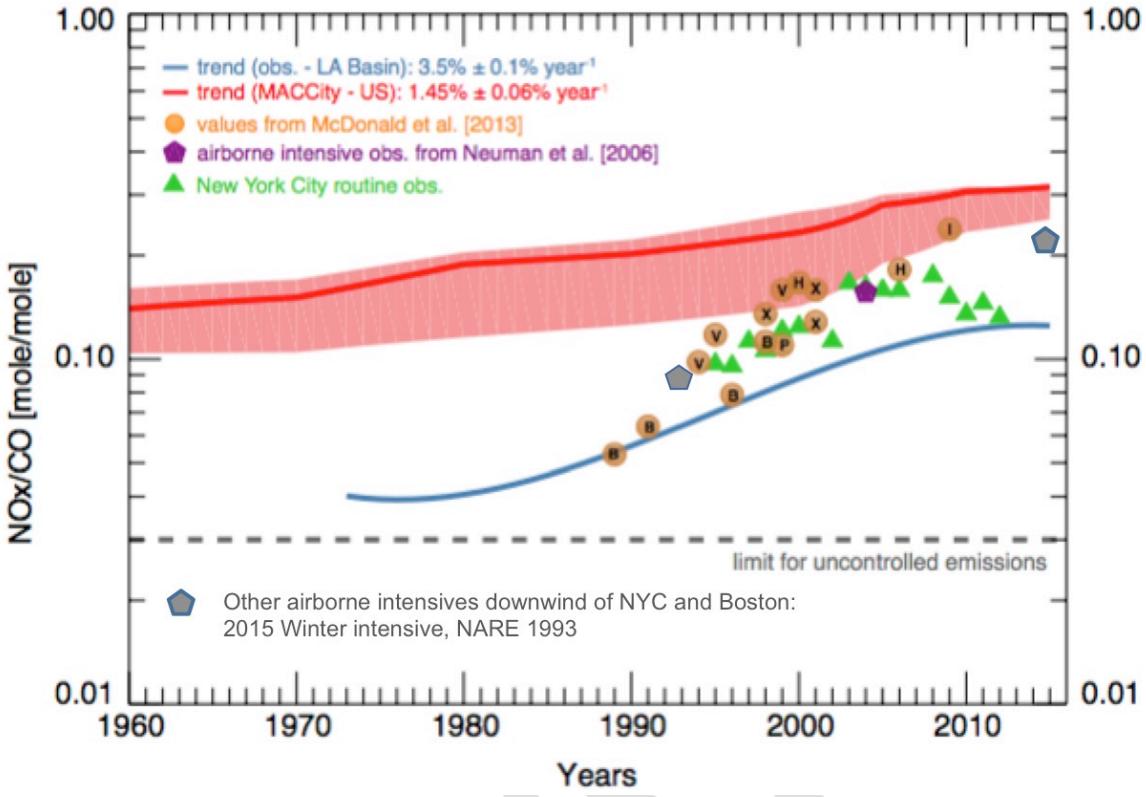

Figure 11. Measured NOx/CO enhancement ratios from the two studies referenced in the figure, from NYC routine monitoring sites, and a trend fit to data from routine monitoring stations in the LA Basin. The pentagons indicate results from airborne field studies downwind of NYC and Boston. The redline indicates the MACCity average NOx/CO total emissions ratios for the entire LA Basin (thick red line) and for each of six model grid cells in the LA Basin (red shading). The NOx/CO ratio for uncontrolled gasoline vehicle emissions (= 0.03) is also shown (dotted gray line). (Figure adapted from *Hassler et al.*, 2016 by M. Trainer, private communication).

The correlation between ozone and CO in transported urban plumes has been taken as a measure of the efficiency of ozone production in those plumes [e.g., *Parrish et al.*, 1993; 1998]. In the 1990s, ozone versus CO slopes of approximately 0.3 to 0.4 mole ozone per mole CO were observed in summer in plumes that had undergone extensive photochemical processing. Figure 12 shows results from

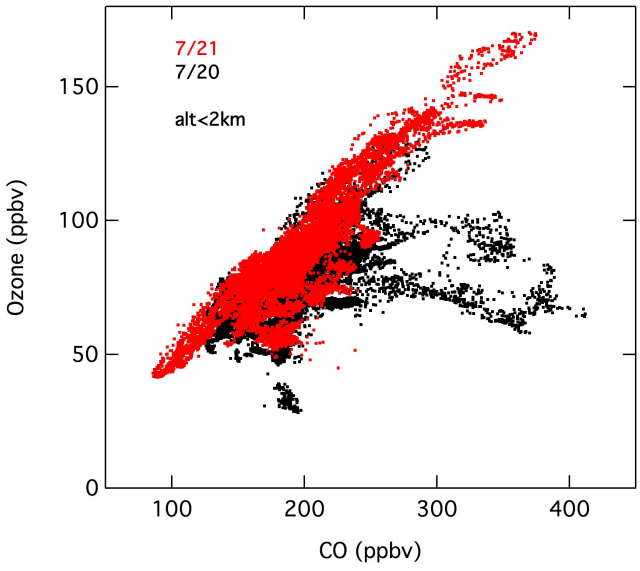

Figure 12. Relationships between ozone and CO measured on two July flights of the NOAA WP-3D aircraft during ICARTT. (Figure prepared by M. Trainer, private communication).

the 20 and 21 July WP-3D flights. During the 21 July flight (red data points) fully processed plumes were sampled, and a slope of 0.57 with a correlation coefficient of R=0.97 was found. Similar slopes were observed during the 20 July flight (black data points), along with smaller slopes and poorer correlations in less well-processed (i.e., fresher) urban plumes. The steeper slopes observed during ICARTT study in 2004 compared to the studies from the 1990s are attributed to differing ozone production efficiencies due to systematic changes that occurred in U.S. urban emissions over the intervening years.

4.0 TOUGHTS ON INTERPRETATIONS OF RECENT DATA COLLECTED IN NORTHEAST U.S.

Approximately 13 years have passed since the ICARTT field study was conducted in 2004. The photochemical environment over and downwind of the New England area has changed over that time in important respects. These changes provide opportunities for insightful analyses, but the analysis techniques discussed in the preceding two sections may have to be adapted to this changed environment. Some particular thoughts in this regard:

- Emissions of CO from motor vehicles have been markedly reduced throughout the U.S. In the ICARTT analysis, CO was used as a marker for transported urban plumes (e.g., Figure 6), since the CO differences between inside and outside such plumes were generally larger than the variability of CO within air masses transported into the region. However, the large reductions in U.S. anthropogenic CO emissions have greatly reduced this utility. During the 2013 SENEX field study conducted in the Southeast U.S., urban plumes, even from cities as large as Atlanta, GA, were often obscured by background CO variability. This change may also affect analyses of data collected in the Northeast U.S.
- Relative emissions of VOCs in U.S. urban areas have been remarkably constant over the past decades (e.g., the discussion of Figure 12 above), and reflect the dominance of automotive emissions. Similarly to CO, automotive emissions of VOCs have been greatly reduced since 2004; thus these relative VOC emission ratios may have systematically changed in ways that reflect the growing relative importance of non-automotive sources of VOCs. Quantification of present emission patterns may provide valuable information regarding the important VOC emission sources.
- Since the ICARTT field study in 2004, urban emissions in the northeastern U.S. have decreased in absolute terms, and the relative rates of emissions of the important ozone precursors have simultaneously changed. These changes are expected to affect the relationships between the ambient concentrations of those precursors (such as shown in Figure 11) and between photochemical products and the precursors (such as shown in Figure 12). Investigation of these systematic changes may provide important information regarding the photochemical environment of the Northeast U.S.

5.0 EXAMINATION OF OZONE DESIGN VALUES IN THE NORTHEAST U.S. - INTRODUCTION, PROCEDURES AND RESULTS

The goal of the remainder of this report is to provide a preliminary examination of the existing record of ozone design values measured in the NESCAUM states (Connecticut, Maine, Massachusetts, New Hampshire, New Jersey, New York, Rhode Island and Vermont) in the widest possible temporal and spatial context. This work comprises the last three tasks of this project:

2. Assemble a historical (1970-2016) archive of Ozone Design Values (ODVs) based on the 2015 ozone NAAQS (i.e., the 3-year average of the annual fourth-highest daily maximum 8-hour average O_3 concentration) for the eight NESCAUM states; these values will be obtained from EPA's AQS and CASTNET archives.
3. Examine the long-term trends of these ODVs to elucidate the relative contributions of local and regional ozone production versus ozone transported into the region. This transported ozone would include contributions from U.S. background ozone (i.e., the ozone transported into the U.S., plus that produced over the U.S. from naturally emitted precursors) and ozone resulting from photochemical processing of U.S. anthropogenic emissions in upwind regions of the Nation.
4. Attempt to estimate U.S. background ozone concentrations in the NESCAUM region by extrapolating long-term trends of observed ODVs to the limit of zero U.S. anthropogenic emissions.

5.1 Historical archive of Ozone Design Values (Task 2)

The historical archive of Ozone Design Values (ODVs) based on the 2015 ozone NAAQS (i.e., the 3-year average of the annual fourth-highest daily maximum 8-hour average O_3 concentration) for the eight NESCAUM states has been assembled. All values were obtained from EPA's AQS data archive. It was verified that data from all of the CASTNET sites in the NESCAUM states are included in the AQS archive. Table 1 gives a descriptive summary of this data set. It should be noted that very few sites have continuous

Table 1. Summary of archive of ODVs for the seven NESCAUM states.

State	sites	years	ODV min# ppb	ODV max# ppb
Connecticut	20	1976-2016	67	169
Maine	32	1978-2016	50	117
Massachusetts	44	1976-2016	56	121
New Hampshire	30	1975-2016	54	104
New Jersey	26	1975-2016	62	132
New York	59	1973-2016	58	129
Rhode Island	4	1978-2016	68	130
Vermont	5	1978-2016	60	96

Excludes a few apparent outliers

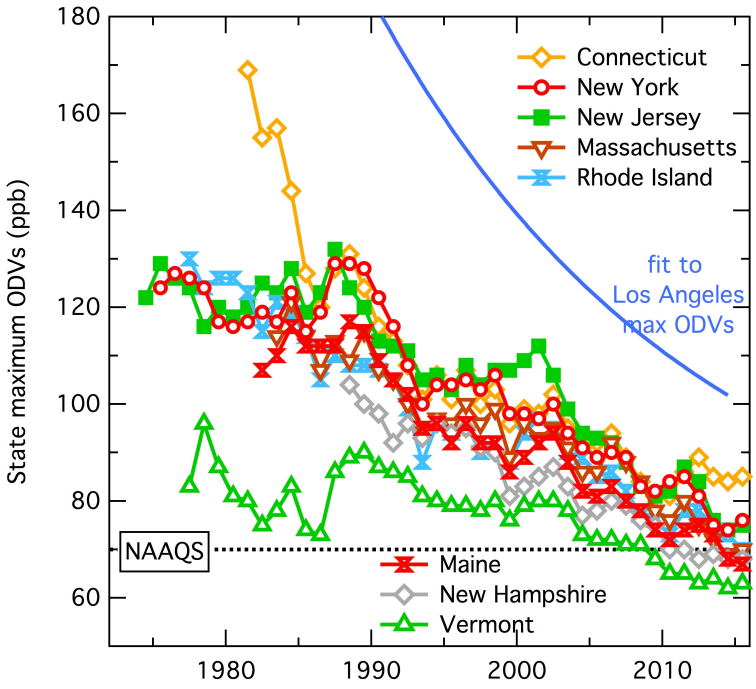

Figure 13. Temporal evolution of the maximum ODV in each of the eight states in the NESCAUM region. A fit to the corresponding evolution in the Los Angeles urban area (i.e., the South Coast Air Basin) is included for comparison. The 2015 National Ambient Air Quality Standard (NAAQS) is also included.

measurements over the complete time span indicated, and that many sites operated for only short periods. All reported ODVs are included in this data archive, even if only a single ODV was reported for a particular site. This data set is available from the author upon request. Figure 13 shows the history of the maximum ODVs observed in each of the eight states included in the NESCAUM region. All of the ODVs recorded in each of those states are plotted in Figures 14-21, along with maps of the monitoring sites.

5.2 Approach for examination of the long-term trends of Ozone Design Values and estimation of U.S. background ozone concentrations

An examination of the long-term trends of ODVs has been completed for southern California air basins [*Parrish et al.,* 2017]. That work utilized an exponential function with a constant positive offset (Equation 1) to quantify the temporal evolution of the ODVs in each air basin:

$$\text{ODV} = y_0 + A \exp\{-(\text{year}-2000)/\tau\}. \qquad (1)$$

Mathematically, the first term of Equation 1, y_0, is the asymptotic value toward which the basin ODVs are approaching, and the second term is the enhancement of the ODVs above y_0, which is assumed to be decreasing exponentially with an e-folding time constant of τ years. Thus, A is the enhancement of the ODVs above y_0 in a reference year, defined here as the year 2000 for this work. *Parrish et al.* [2017] show that a single value of τ (= 21.9 ± 1.2 years), a single value of y_0 (= 62.0 ± 1.9 ppb), and a different value of A in each air basin provided an excellent fit to the maximum ODVs in five of the southern California air basins for the period 1980-2015. The blue line in Figure 13 shows this fit for the Los Angeles urban area (i.e., the South Coast Air Basin). Equation 1 with τ set to 21.9 years will be used here to derive fits to the evolution of ODVs in the NESCAUM region. The utility of these fits to Equation 1 is not justifiable from any rigorous basis (see discussion below), but the resulting fits do provide a basis for quantitative discussion. Two differences between the application here and that of *Parrish et al.* [2017] should be noted. First, the former work considered only the maximum ODV recorded in a year at any site in a given air basin, while

here we consider ODVs from all sites in selected regions. Second, the former work used 1980 as the reference year, while here we use the year 2000; consequently, the A parameters derived here cannot be directly compared with those given for California by *Parrish et al.* [2017].

A conceptual model provides at least a qualitative basis for equation 1. At any given location in the U.S., we can consider ambient ozone concentrations to be composed of two contributions: 1) U.S. background ozone and 2) enhancements resulting from ozone produced from photochemical processing of U.S. anthropogenic emissions of ozone precursors. The first contribution is defined as the ozone that would be present in the absence of U.S. emissions of ozone precursors from anthropogenic sources; this is ozone transported into the U.S., plus that produced over the U.S. from naturally emitted precursors, modified by loss processes. The second contribution accounts for pollution ozone, which can be further divided into two conceptual contributions: pollution ozone transported into a region from upwind U.S. sources, and that produced locally and regionally. We identify the first term of Equation 1, y_0, as the (constant) U.S. background ozone, and the second term as the the sum of the two pollution contributions, which has been decreasing exponentially as emission control efforts have reduced pollution ozone produced from all U.S. anthropogenic emisions. Associating U.S. background ozone with the parameter y_0 is equivalent to extrapolating long-term trends of observed ODVs to the limit of zero U.S. anthropogenic emissions, when the exponential term in Equation 1 equals zero. Using the same value of τ = 21.9 years for the NESCAUM region as for California assumes that control strategies have produced roughly equal relative reductions in ozone precursor emissions throughout the country.

Figure 13 suggests that the conceptual picture described above provides a useful approach. In the NESCAUM region, a general decrease in maximum ozone design values, relatively similar to that seen in California, has occurred, although the maximum concentrations are significantly smaller in the Northeast U.S. The highest Northeast U.S. ODVs are observed in the states that contain the New York City metropolitan area (New York, New Jersey and southwestern Connecticut) or that lie directly downwind (coastal Connecticut). The lowest maximum ODVs are seen in Vermont, which is the only state without major urban areas, and no over-ocean transport path from the New York City area. The ODVs appear to be converging (at least approximately) to a common value in more recent years. Interestingly, Connecticut had much higher ODVs than any other state before 1985; the cause of these much higher values is unknown. Since 1985, Connecticut ODVs have been similar to or somewhat higher than those of other NESCAUM states. In the following section, we fit Equation 1 to the ODVs from selected regions in each of the NESCAUM states. These fits provide the basis for completing Tasks 3 and 4.

5.3 Examination of the long-term trends of Ozone Design Values through fits to Equation 1

Figures 14-21 show all of the ODVs recorded at all sites in each NESCAUM state. The results of fitting Equation 1 to sixteen selected groups of sites within those states are indicated by superimposed curves, and the parameters derived from those fits are given in Table 2. In general, these fits end in 2016 and begin at an earlier year (1990, 1995 or

2000) determined by a subjective determination of a "reasonable" fit to that functional form. Some interesting features of these fits are discussed in this section. The discussion begins first with New York, which is home to the Nation's largest metropolitan center, and then proceeds with the other states roughly in the order of southwest to northeast. Section 6 gives an interpretation of the derived parameters.

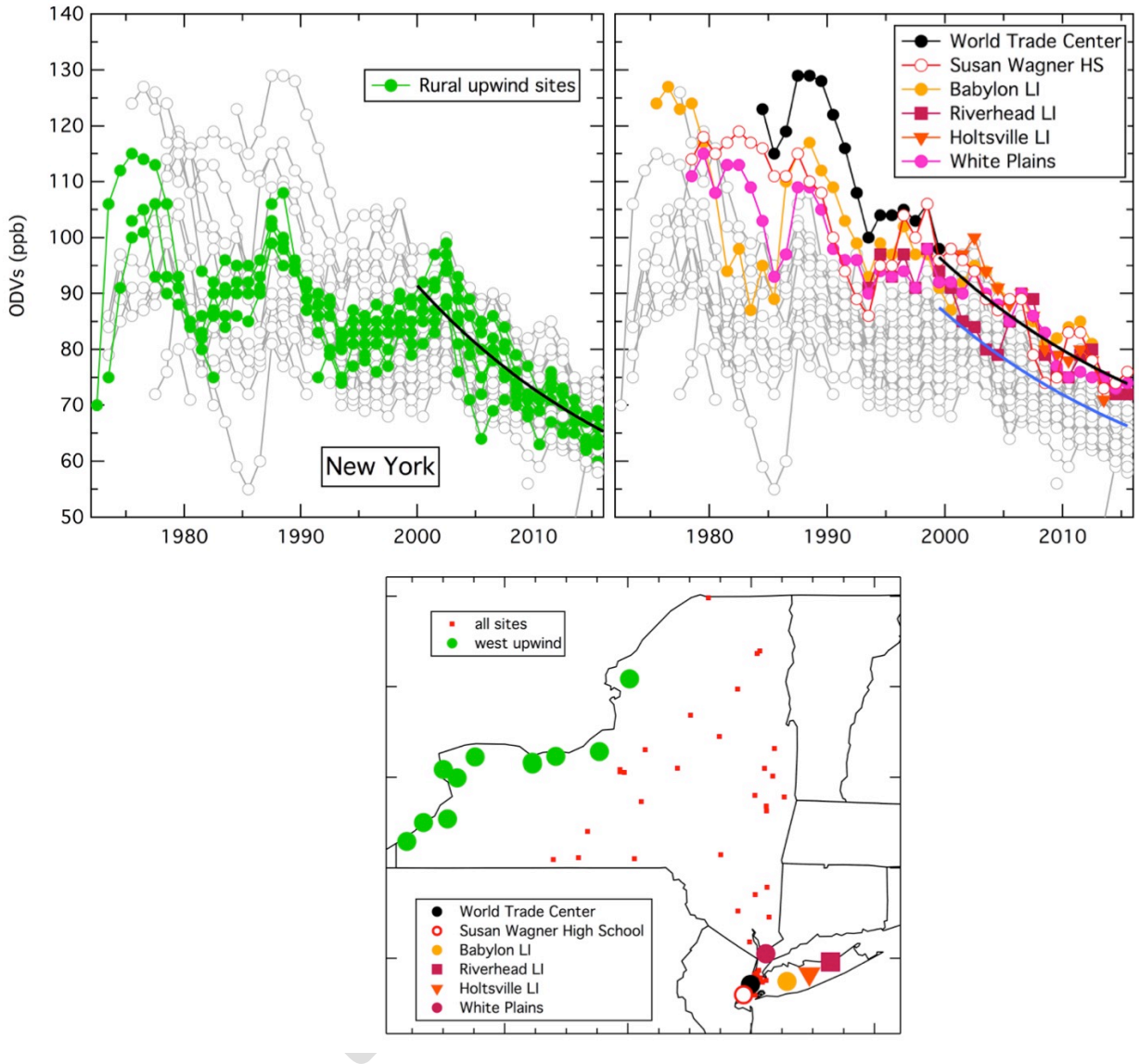

Figure 14. Temporal evolution of the ODVs in New York and map of all monitoring sites reporting ODVs. The upper panels highlight the sites on the western border (left) and the sites with the largest ODVs (right); these sites are also highlighed on the map with corresponding symbols and color-coding. Black curves show fits of Equation 1 for 2000-2016 to the color-coded points in the upper panels; blue curve on right panel shows fit for all ODVs over 2000-2016.

New York has an extensive ozone monitoring network (Figure 14). Early in the measurement record, sites within New York City and on Long Island (highlighted points in the upper right panel) exhibited significantly higher ODVs than other sites. The ODVs at

rural upwind sites (green symbols in upper left panel) on the western border of the state were significantly lower, although in recent years that difference has diminished. Fits to equation 1 for the 2000-2016 period are shown for the two selected sets of sites, as well as for all sites; these curves generally parallel each other.

Figure 15 shows the results for New Jersey. No large differences are seen between the ODVs recorded at any of the sites. The fit of equation 1 to the ODVs recorded in the past 17 years at all sites is included.

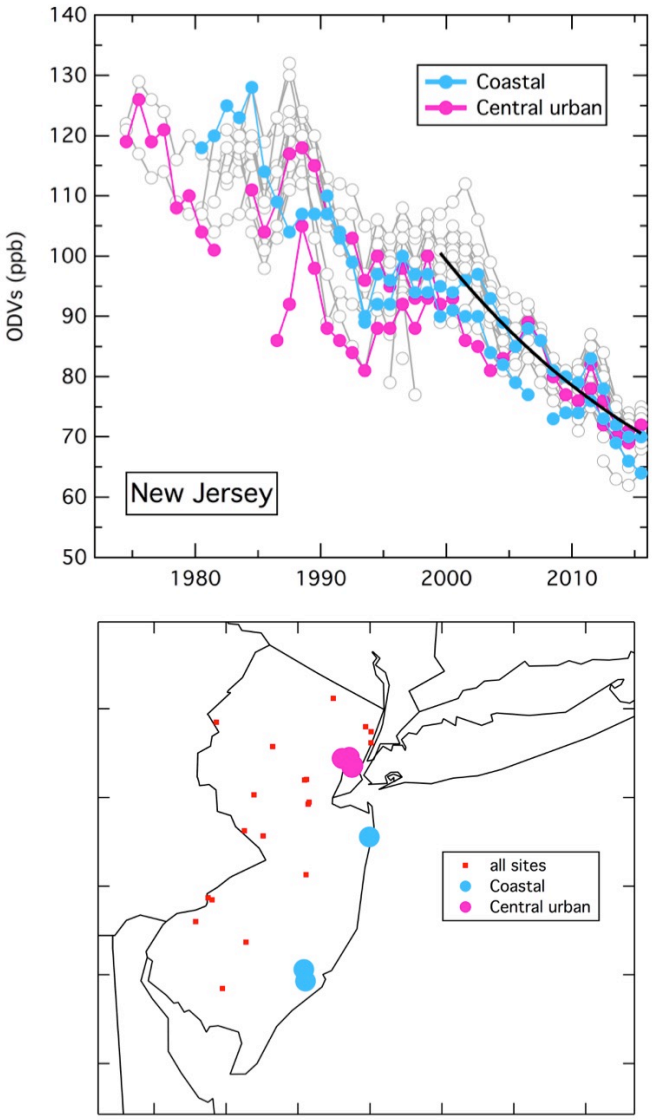

Figure 15. Temporal evolution of the ODVs in New Jersy and map of all monitoring sites reporting ODVs. The two panels highlight the coastal and central urban sites with corresponding symbols and color-coding. A fit of Equation 1 to ODVs from all sites is shown for 2000-2016.

Figure 16 shows the results for Connecticut. Here the largest ODVs are recorded at coastal sites, with the exception of the sites in the urban New Haven area, which has recorded some of the lowest ODVs in the state. This behavior is consistent with transport from the New York City urban area dominating ozone in this state, while fresh NOx emissions in the New Haven region react with this transported ozone, resulting in reduced ODVs in that city. The fit of equation 1 to the ODVs recorded in the past 22 years at all sites is included (solid curve). The dotted curve will be discussed further in Section 6.1.

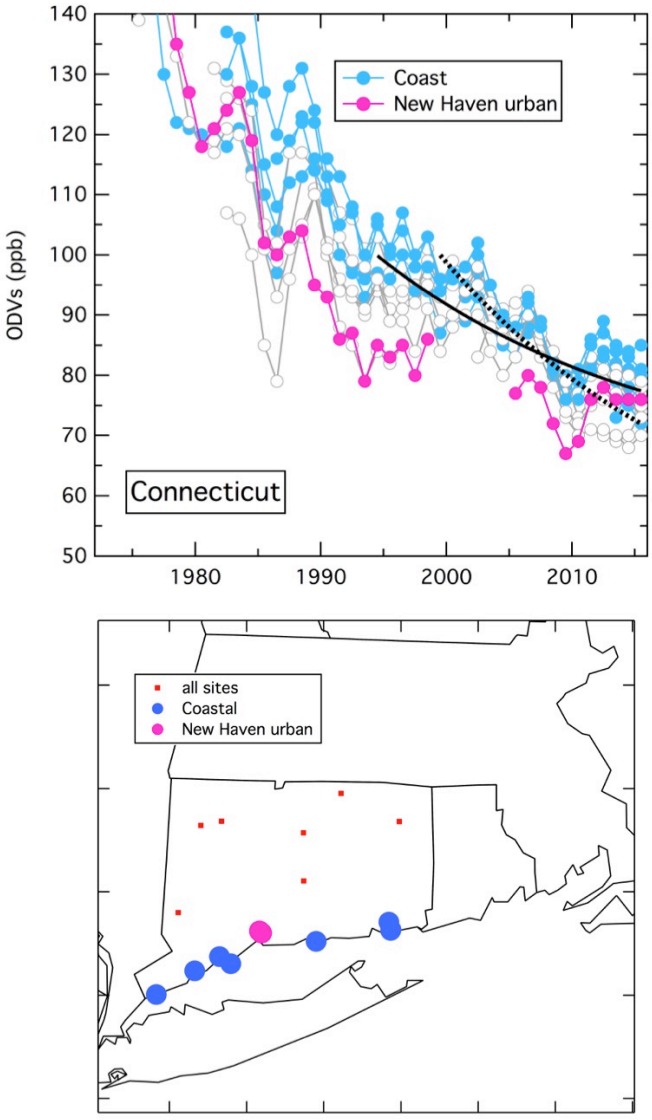

Figure 16. Temporal evolution of the ODVs in Connecticut and map of all monitoring sites reporting ODVs. The two panels highlight the coastal and New Haven urban sites with corresponding symbols and color-coding. A fit of Equation 1 to all ODVs is shown for 1995-2016 (solid curve) and for 2000-2016 with y_0 fixed at 46.0 ppb (dotted curve).

Rhode Island has only a limited ozone monitoring network of four sites (Figure 17). Early in the data record, the inland urban Providence sites recorded lower ODVs then the other two sites, but this difference is largely disappeared. The fit of equation 1 to the ODVs recorded in the past 17 years at all sites is included.

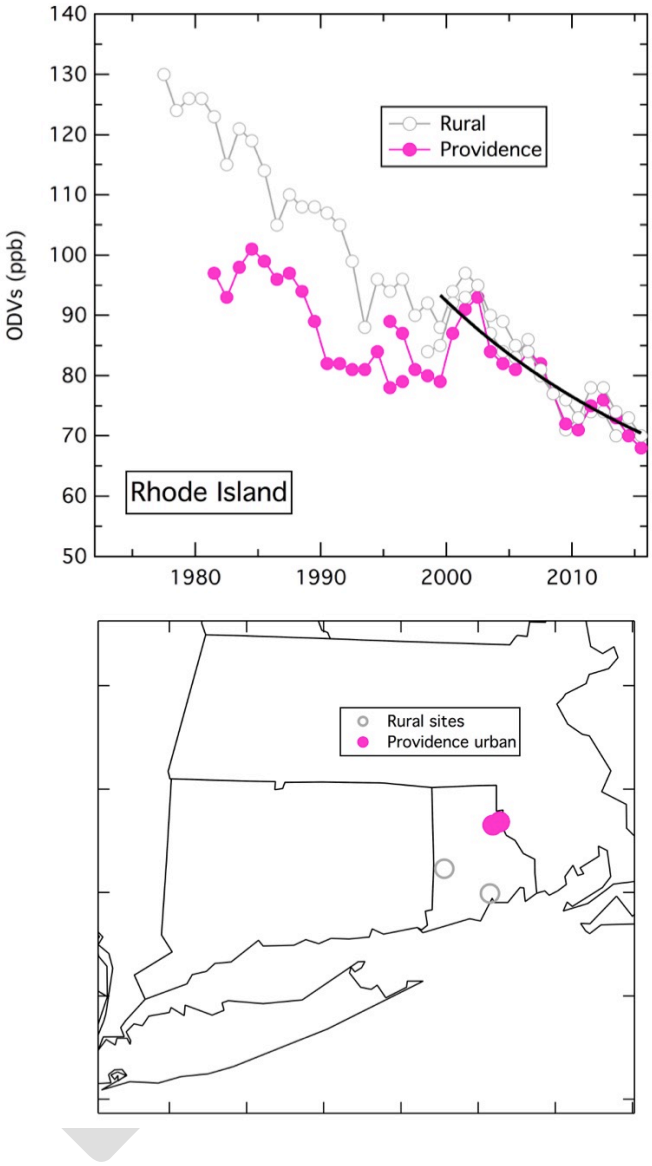

Figure 17. Temporal evolution of the ODVs in Rhode Island and map of all monitoring sites reporting ODVs. The two panels highlight the rural and urban Providence sites with corresponding symbols and color-coding. A fit of Equation 1 to all ODVs is shown for 2000-2016.

Perhaps the most remote coastal sites in the NESCAUM region are located on Martha's Vineyard and Cape Cod, Massachusetts. However, Figure 18 shows that these sites record some of the highest ODVs within that state. This feature emphasizes the important role that transport plays in creating high ozone concentrations well downwind from the East

Coast urban areas. Similar to the situation in Rhode Island, the lowest ODVs are observed in the primary urban area, i.e., Boston in Massachusetts. However, these low values are concentrated only in the center of the urban area, with nearby suburban areas recording ODVs that approach those of the coastal sites. Fits of equation 1 are given for the ODVs recorded at the suburban and coastal sites over the past 17 years, and at the urban sites over the past 27 years.

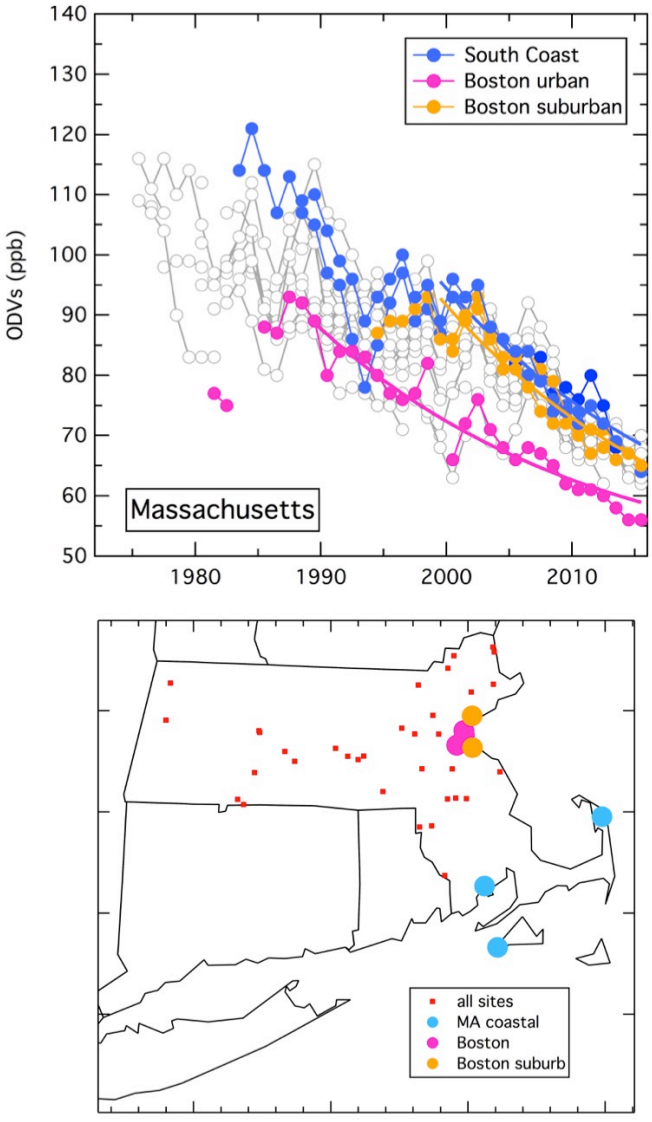

Figure 18. Temporal evolution of the ODVs in Massachusetts and map of all monitoring sites reporting ODVs. The two panels highlight the coastal and Boston urban and suburban sites with corresponding symbols and color-coding. Fits of Equation 1 to the selected ODVs are shown for 2000-2016 for the coastal and suburban sites, and for 1990-2016 for the Boston urban sites.

New Hampshire has established ozone monitoring sites at coastal as well as rural inland locations, plus one on a mountain top (Mt. Washington) at an elevation of 1.9 km. As in Massachusetts, the coastal sites generally record the highest ODVs, with the inland rural sites exhibiting significantly smaller values. Fits of Equation 1 to the coastal and rural sites are over the past 22 and 17 years, respectively, and over the full measurement record (1993-2016) at Mt. Washington. Although the Mt. Washington ODVs are not higher than others recorded in the state, the fit to equation 1 shows a much slower decline than seen at any other site in the NESCAUM region.

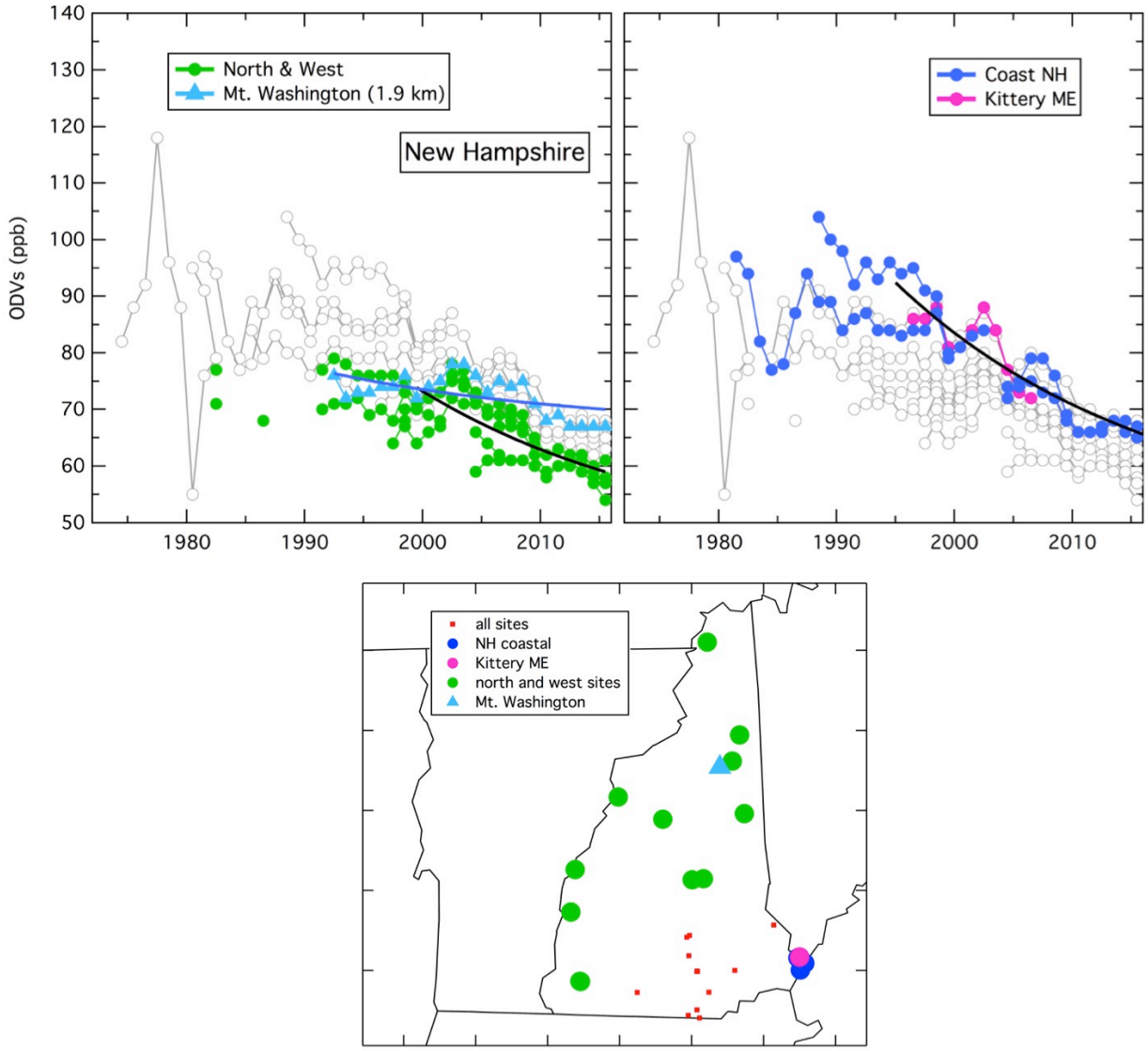

Figure 19. Temporal evolution of the ODVs in New Hampshite and map of all monitoring sites reporting ODVs. The two upper panels highlight the coastal (including Kittery, ME) and the rural north and western sites, including Mt. Washington. The lower panel shows all sites with corresponding symbols and color-coding. Fits of Equation 1 to the selected ODVs are shown for 1995-2016 for the coastal sites, 2000-2016 for the rural sites, and 1990-2016 for the north and western sites; the full data range (1993-2016) is fit for Mt. Washington.

Vermont has a limited ozone monitoring network of five sites at rural locations throughout the state (Figure 20). The fit of equation 1 to the ODVs recorded in the past 17 years at all sites is included in the figure.

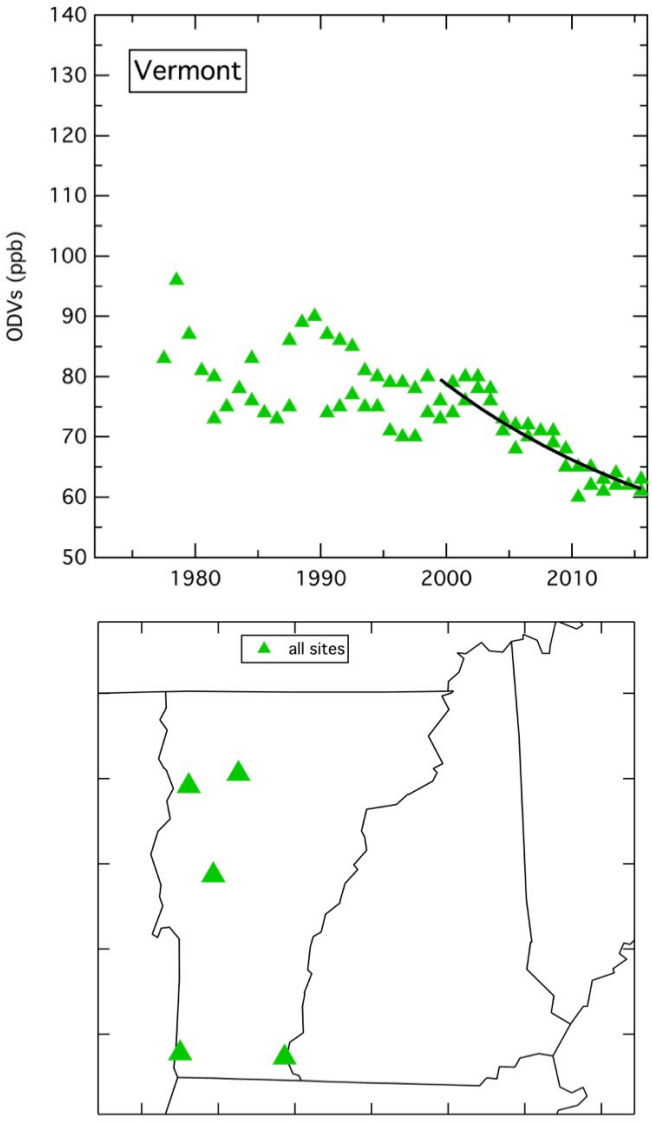

Figure 20. Temporal evolution of the ODVs in Vermont and map of all monitoring sites reporting ODVs. Fit of Equation 1 to all sites is shown for 2000-2016.

Maine has established ozone monitoring at a series of sites along its coast as well as primarily rural inland locations. One coastal site is at a relatively high elevation (0.47 km) on Cadillac Mountain in Acadia National Park. Consistent with states to the southwest, the coastal sites in the southwestern part of the state generally record the highest ODVs, with the northeast coast and the interior rural sites exhibiting significantly smaller values. Fits of Equation 1 to four groups of selected sites are included in Figure 21. These fits generally provide good descriptions of the ODV evolution over longer periods than in other states: 27, 26, 24 and 20 years for the southwest coast, northeast coast, interior sites and Cadillac Mountain, respectively. These periods cover the complete records from the northeast coast and Cadillac Mountain. In contrast to the fit to Mt. Washington ODVs, the Cadillac Mountain record is in close accord with the other southwest coastal sites, although those ODVs appear to be somewhat higher than others recorded at the southwest coastal sites, features consistent with sampling air from higher altitudes within the MBL.

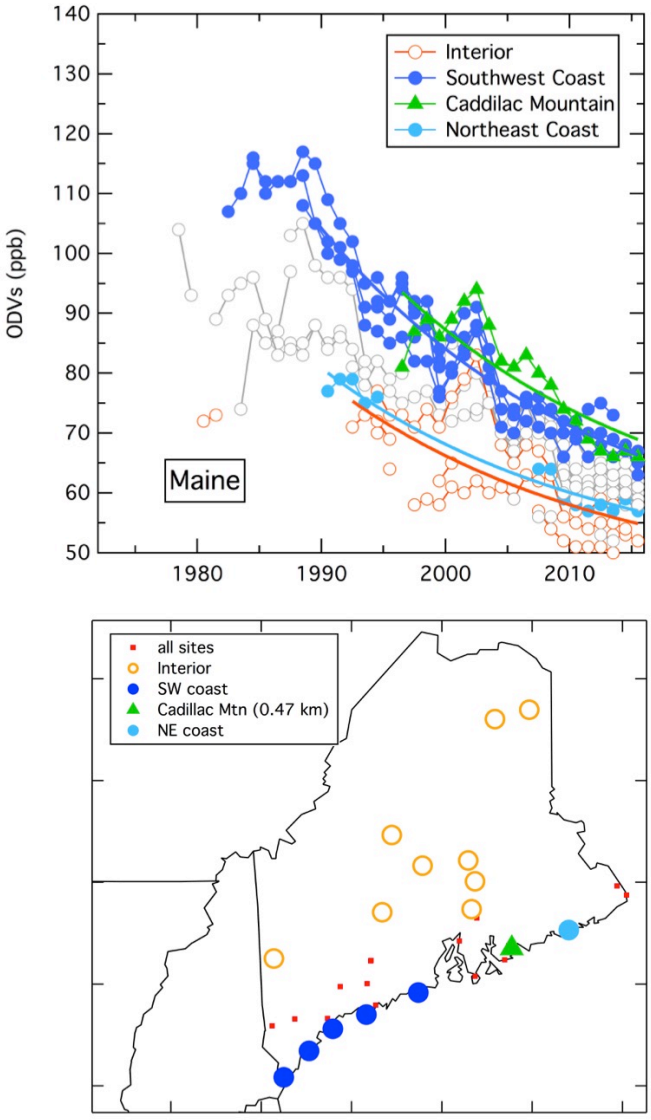

Figure 21. Temporal evolution of the ODVs in Maine and map of all monitoring sites reporting ODVs. Fits of Equation 1 to four sets of sites are shown.

Table 2. Results of least-squares fits to Equation 1 illustrated in Figures 14-21. The absolute root-mean-square deviations between the observed ODVs and the derived fits (σ) are indicated.

State/sites	years fit	y_0 (ppb)	A (ppb)	σ (ppb)	A^* (ppb)
New York/maximum	2000-2016	53 ± 7	44 ± 10	4.0	53 ± 2
New York/rural upwind	2000-2016	41 ± 7	50 ± 10	5.1	44 ± 2
New Jersey/all sites	2000-2016	43 ± 5	58 ± 6	4.6	53 ± 2
Connecticut/all sites	1995-2016	63 ± 5	29 ± 5	5.8	54 ± 2
Rhode Island/all sites	2000-2016	49 ± 9	44 ± 13	4.1	54 ± 2
Massachusetts/Boston	1990-2016	46 ± 7	27 ± 7	3.2	27± 2
Massachusetts/suburban	2000-2016	41 ± 10	52 ± 14	3.3	45 ± 3
Massachusetts/coastal	2000-2016	43 ± 10	52 ± 13	3.2	49 ± 3
New Hampshire/coastal	1995-2016	49 ± 7	35 ± 8	3.7	38 ± 2
New Hampshire/northwest	2000-2016	45 ± 7	29 ± 9	3.7	28 ± 2
New Hampshire/Mt. Washington	1993-2016	67 ± 7	7 ± 8	3.0	---
Vermont /all sites	2000-2016	44 ± 8	35 ± 10	2.7	33 ± 2
Maine/interior	1993-2016	44 ± 9	23 ± 10	5.8	20 ± 3
Maine/NE coast	1991-2016	46 ± 5	22 ± 5	1.9	23 ± 2
Maine/SW coast	1990-2016	49 ± 5	36 ± 5	4.1	39 ± 2
Maine/Cadillac Mtn.	1997-2016	51 ± 17	37 ± 13	5.3	43 ± 5

* Derived from fit with y_0 set equal to 46 ppb.

5.4 Confidence limits for the parameters derived in the fits to Equation 1

Table 2 gives a confidence limit for each of the derived parameters. These are the 95% confidence limits derived from the least-squares fitting routine that have been adjusted to account for the known covariance between the recorded ODVs. Each ODV is a three-year running mean; therefore only every third ODV is completely independent from the others determined at a given site. Consequently, the number of independent variables in each fit is approximately a factor of three smaller than the number of ODVs reported from the selected group of sites. Thus, the fitting routine underestimates the true confidence limits of the derived parameters. In Table 2, all derived confidence limits have been increased by a factor of $3^{1/2}$ to account for this covariance, giving more realistic confidence limits.

There are additional sources of covariance between the ODVs included in any particular fit. The ODVs from different sites within a particular region often co-vary due to regional interannual variability. Also temporal interannual variability at a given site may well lead to covariance between ozone concentrations measured in successive years at that site. We are not able to account for the effect of this additional covariance; the confidence limits in Table 2 must be considered as lower limits to the true confidence limits of the derived parameters.

6.0 INTERPRETATIONS OF ODV LONG-TERM TRENDS

The goal of this section is to synthesize the results of the fits to the long-term trends of the ODVs derived in Section 5.3, and to extract general information regarding the temporal and spatial variability of ODVs in the NESCAUM region. The parameters of the derived ODV fits are summarized in Table 2. Considerable similarity, with some notable differences, is apparent between the fits of the different selections of sites in the eight states. Figure 22 compares all of the fits (except for the dotted curve in Figure 16, which is discussed below) by plotting them on the same graph. Except for the two fits denoted by the colored curves, all appear to be similar in the sense that they exhibit the same relative long-term decrease and are approaching a common value of y_0. The same relative long-term decrease is necessarily forced by the use of the same value of τ = 21.9 years in all fits. However, the derived A and y_0 values do provide useful information regarding the spatial and temporal variation of ODVs over the past two to three decades in the NESCAUM region.

6.1 Estimation of the U.S. background ODVs in the NESCAUM region

The parameters of the fits given in Table 2 provide a quantitative basis for judging the similarity of the fits throughout the eight NESCAUM states. The average of all y_0 values (excluding the two exceptions indicated in Figure 22) is 46.1 ppb with a standard deviation of 3.7 ppb. An average of these y_0 values weighted with the inverse square of the respective confidence limits is 46.0 ± 1.8 ppb, where the 95 % confidence of this average is indicated. It is encouraging to note that all of the y_0 values in table 2 agree (with the two exceptions noted above) within their indicated confidence limits, with these average derived values.

Recalling the discussion in Section 5.2, we identify $y_{0,}$ as the U.S. background ODV, i.e. the ODV expected if U.S. anthropogenic emissions were reduced to zero. We take the latter value of y_0 = 46.0 ± 1.8 ppb as the best estimate of this U.S. background ODV in the NESCAUM region. This is significantly smaller than the value of 62.0 ± 1.9 ppb derived for southern California [*Parrish et al.,* 2017]. As a consequence the NESCAUM region has a much larger margin for enhancements of ODVs while still attaining the 2015 NAAQS of 70 ppb.

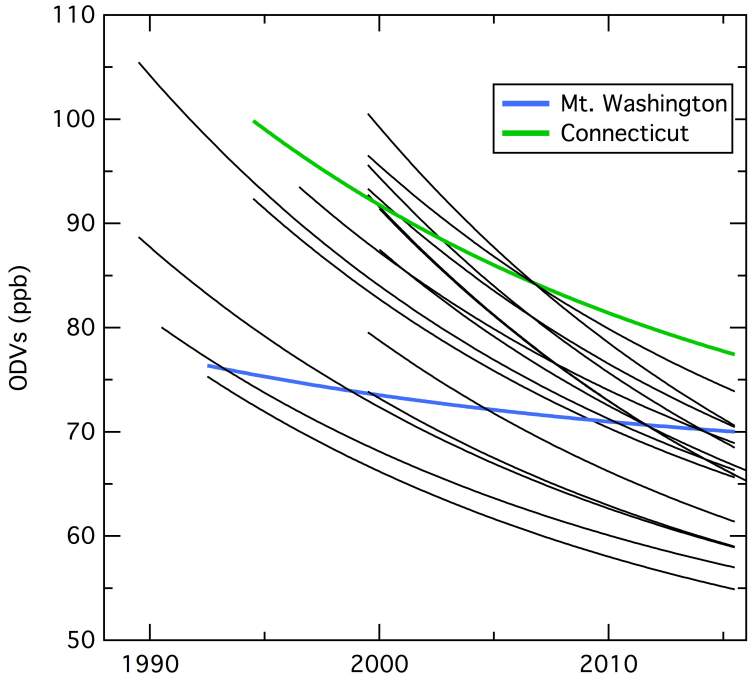

Figure 22. Comparison of fits of Equation 1 to the ODVs shown in Figures 14-21. The parameters of these fits are included in Table 2.

It should be recognized that the derived y_0 values are sensitive to the selected τ value, with a larger value of τ giving a lower value for y_0, and vice versa. For example, using the Boston data from Figure 18, increasing the assumed value of τ by 10% (from 21.9 to 24.1 years) decreases the derived y_0 estimate by 6% (from 45.8 to 43.3 ppb). It is not clear how the time scale of California emission reductions compare to that in the NESCAUM region. In California, reductions may have been faster because that state may have had more aggressive emission control measures, but they may also have been slower because controls on eastern coal-fired power plants have dramatically reduced NOx emissions, while this would not have occurred in California where such power generation is located downwind, out-of-state. On the other hand, emission reduction rates could be roughly the same, as many Northeast states have adopted the California mobile source emission control program. Regardless, fixing the value of τ at 21.9 years means that the confidence limits derived in this analysis are necessarily lower limits, and the derived values of y_0 and A are more uncertain than these confidence limits indicate.

6.2 Estimation of the year 2000 enhancement of ODVs in the NESCAUM region

Estimates of A, the enhancements of the ODVs above y_0 in the reference year 2000, are available from the fits to Equation 1 with τ = 21.9 years. Table 2 lists these values from the two parameter fits, i.e., with y_0 and A as independent parameters determined from the least-squares fits. The discussion in Section 6.1 establishes that a constant value of y_0 = 46.0 ± 1.8 ppb is a useful estimate for the entire NESCAUM region. In this case, we can derive one parameter fits to Equation 1 with y_0 held constant at this value; the results of these fits are included in Table 2 as the A^* values. (Such a fit is not done for the Mt. Washington results as discussed below.) The A^* values generally agree with the A values from the two parameter fits within their confidence limits, but have smaller confidence limits, since only one parameter need be derived. One exception to the agreement between A and A^* is the fit to the Connecticut sites; this A value is anomalously low, and A^* agrees more closely with the corresponding values in the neighboring states of New Jersey and New York. Thus, we use the A^* value for that state in the following analysis.

An overview of the spatial variation of the ODV enhancements across the NESCAUM region can be obtained from a contour plot of the A^* values (upper panel of Figure 23). The groups of selected sites fit to Equation 1 give only very coarse spatial resolution across the NESCAUM region; thus it must be fully appreciated that the contour plot has large uncertainties not apparent from the smooth spatial variability of the figure. Additional subjectivity is introduced by the inclusion of duplicated values added to the contouring program to ensure that the contours reproduce expected features. Nevertheless, the plot does give a reliable, semi-quantitative representation of the enhancement of ODVs and its regional variation in the year 2000.

It must also be appreciated that the A and A^* values and Figure 23 describe the situation as it was in the year 2000. As is apparent from Figures 13-22, ODVs have decreased throughout the last several decades in the NESCAUM region. We have used an e-folding time of τ = 21.9 years to represent this decrease. This implies that between the reference year of 2000 and the present, the ODV enhancements have decreased by more than a factor

of 2. Hence, dividing the ODVs in Figure 23 by 2 gives an approximation of present-day ODVs.

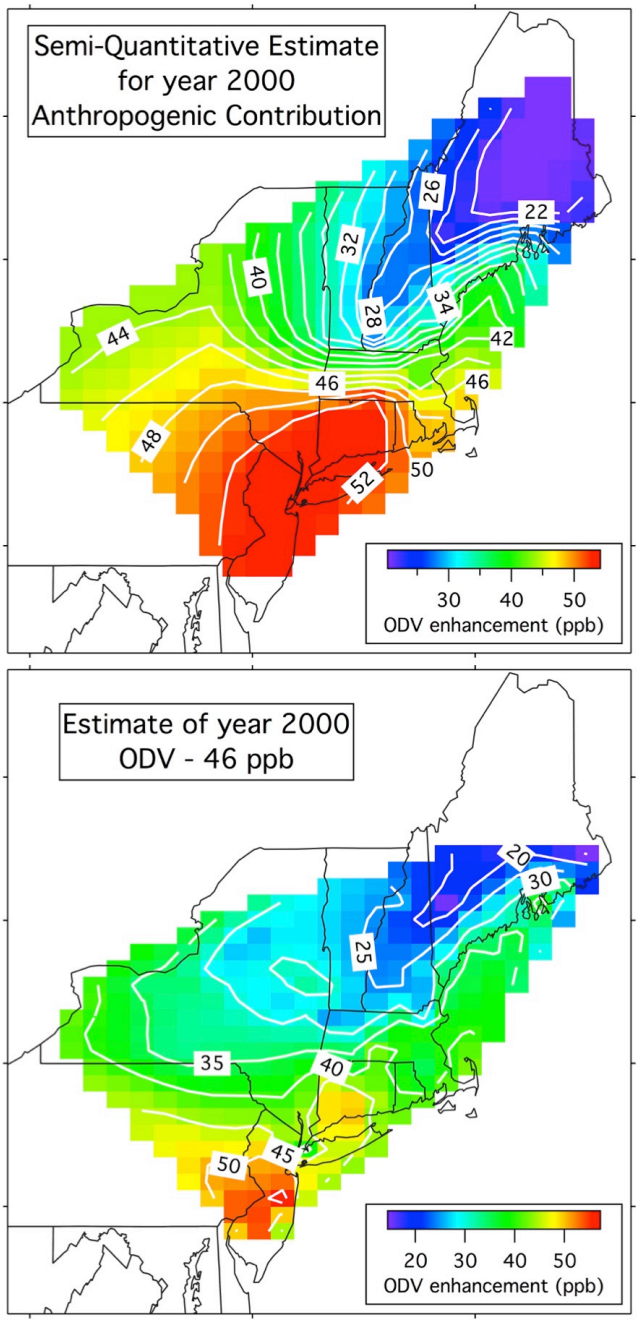

Figure 23. Contour plots of the enhancement of ozone design values in the NESCAUM region due to photochemical production from anthropogenic emissions. In the upper panel these quantities are estimated for the regions of the selected sites from the A^* values from Table 2. In the lower panel they are estimated from the ODVs recorded at individual sites in the year 2000 with y_0 = 46 ppb subtracted.

A contour plot of the spatial variation of the ODV enhancement in the year 2000 can also be derived directly from the year 2000 ODVs reported throughout the NESCAUM region. Here, the value of y_0 = 46 ppb is simply subtracted from the station ODVs reported in that year, and a contour plot derived. The lower panel of Figure 23 shows the result of this procedure. The plots show a great deal of similarity, but there are some differences. These differences largely represent 1) the particular meteorological features of the year 2000, while the A^* contour map represents a more average situation, 2) noise from interannual variability of the ODVs recorded in any given year, and 3) the lack of inclusion of duplicative values to ensure that the contours reproduce expected features.

Finally, Figure 22 indicates that the ODVs recorded at the one high elevation site (Mt. Washington at 1.9 km) in the region have followed a temporal evolution different from any of the other sites. The A value (7 ± 8 ppb) is much smaller than that of any of the selected sets of sites, and the U.S. background ODV (y_0 = 67 ± 7 ppb) is significantly higher than the common τ by 10% (from 21.9 to 24.1 years appropriate for the entire NESCAUM region). This difference is believed to reflect the behavior of ozone in the free troposphere over the northeastern U.S. Ozone concentrations in the free troposphere increase with altitude (Figures 4 and 6) and it is these higher altitude ozone air parcels that impact Mt.

Washington. The value of y_0 at Mt. Washington is in reasonable accord with the average ozone concentrations measured over the eastern U.S. by the MOZAIC program in the years near 2000 (Figure 4).

6.3 Final thought on interpretation of the analysis presented.

The analysis presented in Sections 5 and 6 of this report provides a conceptualization of the temporal and spatial distribution of the ozone design values in the NESCAUM region. This analysis is based on two assumptions: first, the time constant for the exponential decrease of ODVs in California (i.e., τ = 21.9 years) is assumed also to be appropriate for this region of the country, and second, a uniform U.S. background ODV (i.e., y_0 = 46.0 ± 1.8 ppb) applies to the entire region. These two assumptions are plausible but unproven; thus, the results presented here should be considered more as a useful guide for further thought, and less as a definitive quantification of that temporal and spatial distribution.

7.0 REFERENCES

Angevine, W. M., J. E. Hare, C. W. Fairall, D. E. Wolfe, R. J. Hill, W. A. Brewer, and A. B. White (2006), Structure and formation of the highly stable marine boundary layer over the Gulf of Maine, J. Geophys. Res., 111, D23S22, doi:10.1029/2006JD007465.

Baker, A. K., A. J. Beyersdorf, L. A. Doezema, A. Katzenstein, S. Meinardi, I. J. Simpson, D. R. Blake, and F. S. Rowland (2008), Measurements of nonmethane hydrocarbons in 28 United States cities, Atmos. Environ., 42(1), 170–182, doi:10.1016/j.atmosenv.2007.09.007.

Fehsenfeld, F. C., et al. (2006), International Consortium for Atmospheric Research on Transport and Transformation (ICARTT): North America to Europe—Overview of the 2004 summer field study, J. Geophys. Res., 111, D23S01, doi:10.1029/2006JD007829.

Hassler, B., et al. (2016), Analysis of long-term observations of NO_x and CO in megacities and application to constraining emissions inventories, Geophys. Res. Lett., 43, 9920–9930, doi:10.1002/2016GL069894.

Lee, S.-H., et al. (2011), Modeling ozone plumes observed downwind of New York City over the North Atlantic Ocean during the ICARTT field campaign, Atmospheric Chemistry and Physics, 11(15), 7375-7397, doi:10.5194/acp-11-7375-2011.

Neuman, J. A., et al. (2006), Reactive nitrogen transport and photochemistry in urban plumes over the North Atlantic Ocean, J. Geophys. Res., 111, D23S54, doi:10.1029/2005JD007010.

Parrish, D.D., J.S. Holloway, M. Trainer, P.C. Murphy, G.L. Forbes, and F.C. Fehsenfeld (1993), Export of North American Ozone Pollution to the North Atlantic Ocean, Science, 259, 1436-1439.

Parrish, D.D., M. Trainer, J.S. Holloway, J.E. Yee, M.S. Warshawsky, F.C. Fehsenfeld, G.L. Forbes, and J.L. Moody (1998), Relationships between ozone and carbon monoxide at surface sites in the North Atlantic region, J. Geophys. Res., 103(D11), 13357–13376, doi:10.1029/98JD00376.

Parrish, D.D., L.M. Young, M.H. Newman, K.C. Aikin and T.B. Ryerson (2017), *J. Geophys. Res. Atmos.,* in press. (Manuscript copy available upon request.)

Warneke, C., et al. (2006), Biomass burning and anthropogenic sources of CO over New England in the summer 2004, J. Geophys. Res., 111, D23S15, doi:10.1029/2005JD006878.

Warneke, C., et al. (2007), Determination of urban volatile organic compound emission ratios and comparison with an emissions database, J. Geophys. Res., 112, D10S47, doi:10.1029/2006JD007930.

White, A. B., L. S. Darby, C. J. Senff, C. W. King, R. M. Banta, J. Koermer, J. M. Wilczak, P. J. Neiman, W. M. Angevine, and R. Talbot (2007), Comparing the impact of meteorological variability on surface ozone during the NEAQS (2002) and ICARTT (2004) field campaigns, J. Geophys. Res., 112, D10S14, doi:10.1029/2006JD007590.